

# ON THE STABILITY OF APPROXIMATE DISPLACED LUNAR ORBITS

Jules Simo\* and Colin R. McInnes†

In a prior study, a methodology was developed for computing approximate large displaced orbits in the Earth-Moon circular restricted three-body problem (CRTBP) by the Moon-Sail two-body problem. It was found that far from the  $L_1$  and  $L_2$  points, the approximate two-body analysis for large accelerations matches well with the dynamics of displaced orbits in relation to the three-body problem. In the present study, the linear stability characteristics of the families of approximate periodic orbits are investigated.

## INTRODUCTION

The design of spacecraft trajectories is a crucial task in space mission design. Solar sail technology appears to be a promising form of advanced spacecraft propulsion which can enable exciting new space-science mission concepts for solar system exploration and deep space observation. Although solar sailing has been considered as a practical means of spacecraft propulsion only relatively recently, the fundamental ideas are by no means new (see McInnes<sup>1</sup> for a detailed description). A solar sail is propelled by reflecting solar photons and therefore can transform the momentum of the photons into a propulsive force. Solar sails can also be utilised for highly non-Keplerian orbits, such as orbits displaced high above the ecliptic plane (see Waters and McInnes<sup>2</sup>). Solar sails are especially suited for such non-Keplerian orbits, since they can apply a propulsive force continuously. In such trajectories, a sail can be used as a communication satellite for high latitudes. For example, the orbital plane of the sail can be displaced above the orbital plane of the Earth, so that the sail can stay fixed above the Earth at some distance, if the orbital periods are equal (see Forward<sup>3</sup>). Orbits around the collinear points of the Earth-Moon system are also of great interest because their unique positions are advantageous for several important applications in space mission design (see e.g. Szebehely<sup>4</sup>, Roy,<sup>5</sup> Vonbun,<sup>6</sup> Gómez et al.<sup>7</sup>). In recent years several authors have tried to determine more accurate approximations (quasi-Halo orbits) of such equilibrium orbits<sup>8</sup>. These orbits were first studied by Farquhar<sup>9</sup>, Farquhar and Kamel<sup>8</sup>, Breakwell and Brown<sup>10</sup>, Richardson<sup>11</sup>, Howell<sup>12</sup>. If an orbit maintains visibility from Earth, a spacecraft on it (near the lunar  $L_2$  point) can be used to provide communications between the equatorial regions of the Earth and the lunar far-side. The establishment of a bridge for radio communications is crucial for forthcoming space missions, which plan to use the lunar poles. McInnes<sup>13</sup> investigated a new family of displaced solar sail orbits near the Earth-Moon libration points. Displaced orbits have more recently been developed by Ozimek et al.<sup>14</sup> using collocation methods for lunar south pole communications. In Baoyin and McInnes<sup>15</sup> and McInnes<sup>13,16</sup>, the authors describe new orbits which are associated with artificial Lagrange points in the Earth-Sun system. These artificial equilibria also have potential applications for future space

\*Research Fellow, Advanced Space Concepts Laboratory, Department of Mechanical Engineering, University of Strathclyde, Glasgow, G1 1XJ, United Kingdom. Email: jules.simo@strath.ac.uk.

†Professor, Advanced Space Concepts Laboratory, Department of Mechanical Engineering, University of Strathclyde, Glasgow, G1 1XJ, United Kingdom. Email: colin.mcinnnes@strath.ac.uk.

physics and Earth observation missions (see Scheeres<sup>17</sup>). In McInnes and Simmons<sup>18</sup>, the authors investigate large new families of solar sail orbits, such as Sun-centered halo-type trajectories, with the sail executing a circular orbit of a chosen period above the ecliptic plane. We have recently investigated displaced periodic orbits at linear order in the Earth-Moon restricted three-body system, where the third massless body is a solar sail (see Simo and McInnes<sup>19</sup>). These highly non-Keplerian orbits are achieved using an extremely small sail acceleration. It was found that for a given displacement distance above/below the Earth-Moon plane it is easier by a factor of order 3.19 to do so at  $L_4/L_5$  compared to  $L_1/L_2$  - ie. for a fixed sail acceleration the displacement distance at  $L_4/L_5$  is greater than that at  $L_1/L_2$ . In addition, displaced  $L_4/L_5$  orbits are passively stable, making them more forgiving to sail pointing errors than highly unstable orbits at  $L_1/L_2$ . The drawback of the new family of orbits is the increased telecommunications path-length, particularly the Moon- $L_4$  distance compared to the Moon- $L_2$  distance.

The solar sail Earth-Moon problem differs greatly from the Earth-Sun system as the Sun-line direction varies continuously in the rotating frame and the equations of motion of the sail are given by a set of nonlinear, non-autonomous ordinary differential equations. Trajectories near the Earth-Moon  $L_1$  and  $L_2$  points are not easily identified, such that the solar sail can enable continuous communications with the equatorial regions of the Earth from any point on the lunar far-side. We therefore developed an asymptotic analysis for large ( $a_0 = 1.7 \text{ mm/s}^2$ ) and small ( $a_0 = 0.58 \text{ mm/s}^2$ ) accelerations (see Simo and McInnes<sup>20</sup>). This analysis is obtained within an approximation of large displaced orbits ( $a_0 = 1.7 \text{ mm/s}^2$ ) by the Moon-Sail two-body problem. The displaced periodic orbits found approach the asymptotic solutions as the characteristic acceleration becomes large. It is shown for example that, with a suitable sail attitude control program, a  $4 \times 10^4 \text{ km}$  displaced, out-of-plane trajectory far from the  $L_2$  with a sail acceleration of  $1.7 \text{ mm/s}^2$  can be approximated using the two-body analysis.<sup>20</sup> This simple, two-body approximate analysis matches with the large displaced orbits found by Ozimek et al.<sup>14</sup> using numerical collocation methods in a previous study. For small accelerations we use a linear approximation of the Earth-Moon three-body problem which again matches well with Ozimek et al.<sup>14</sup>

Throughout the paper we consider the dynamics of displaced orbits in relation to an approximate two-body Earth-Moon problem with a constant radiation pressure. The aim of the present paper is to develop a method to study the stability of approximate displaced two-body lunar orbits to obtain analytic insights into their stability properties. Building on earlier work of McInnes,<sup>21</sup> an analogue proof of stability analysis of displaced two-body lunar orbits will be derived. In order to carry out a linear stability analysis, we then perturb the system and analyse the resulting dynamics.

## METHODOLOGY

### Basic Definitions

In this section, we consider the motion of a solar sail moving under the gravitational influence of the Moon only as shown in Figure 1 (a). Such a problem is defined as the approximate Moon-Sail two-body problem. For a large displacement, such that the sail is far from the  $L_1$  or  $L_2$  point this provides a remarkably good approximation to the problem. The forces acting on the sail can be seen in Figure 1 (b).

In this model, the Moon is assumed to be fixed, while the solar sail is in a rotating frame of reference. To describe the motion of the sail, we take a reference frame rotating with the Sun-line at angular velocity  $\omega_*$ , such that the origin is at the center  $c$ , as shown in Figure 1 (a). From the

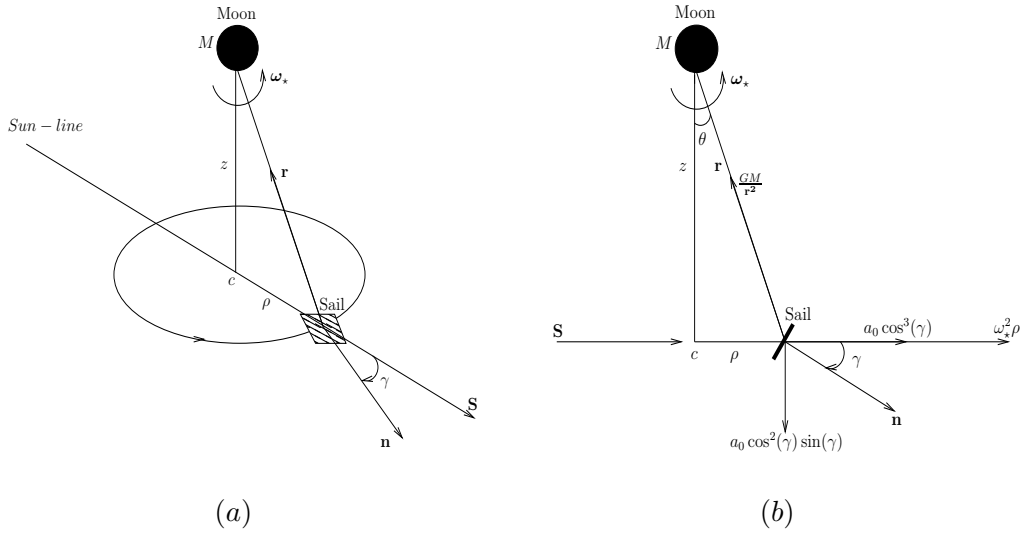


**Figure 1** (a) Schematic geometry of the Moon-Sail two-body problem generating a hover orbit displaced below Earth-Moon plane for lunar south pole communications; (b) Representative forces.

perspective of an inertial reference frame, Figure (2) shows the Moon and the sail orbiting around the Earth.

### System Dynamics

The equation of motion of the sail in a rotating frame of reference is described by

$$\frac{d^2 \mathbf{r}}{dt^2} + 2\boldsymbol{\omega}_* \times \frac{d\mathbf{r}}{dt} + \nabla \tilde{U}(\mathbf{r}) = \mathbf{a}, \quad (1)$$

where  $\boldsymbol{\omega}_* = \omega_* \hat{\mathbf{z}}$  ( $\hat{\mathbf{z}}$  is a unit vector pointing in the direction of  $\mathbf{z}$ ) is the angular velocity vector of the rotating frame and  $\mathbf{r}$  is the position vector of the solar sail to the central body. This frame of reference rotates with constant angular velocity relative to an inertial frame.

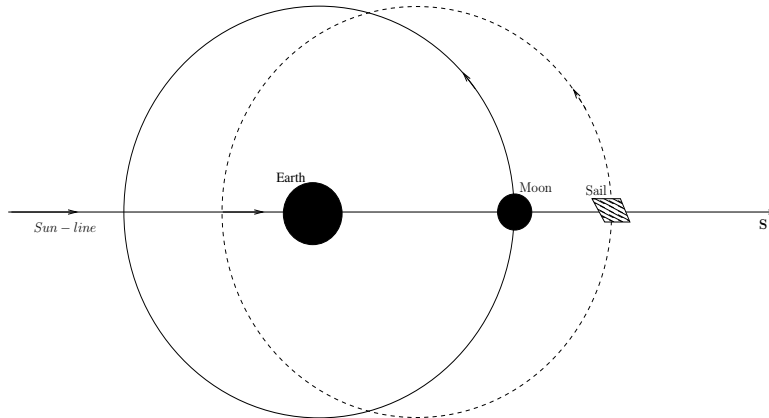


**Figure 2** Schematic geometry of the Moon-Sail two-body orbiting around the Earth (Inertial Frame).

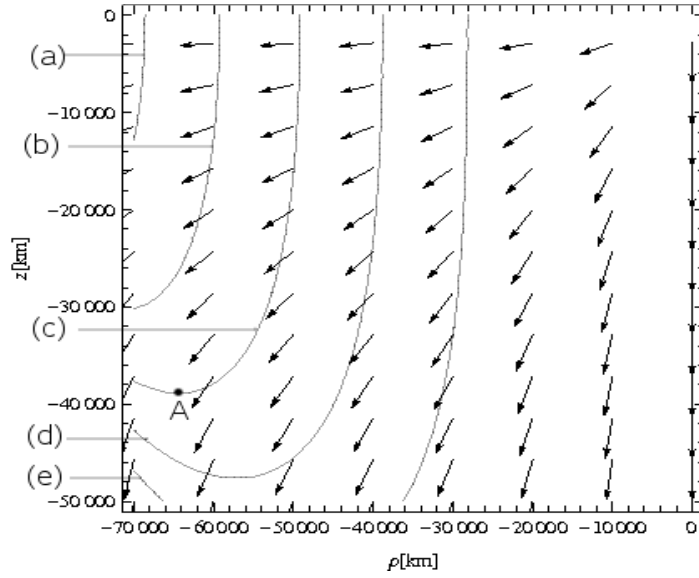


**Figure 3** A contour plot and the vector field of the characteristic acceleration  $a_0 = a_0(\rho, z)$  in the Earth-Moon system: (a)  $a_0 = 0.58 \text{ mm/s}^2$ , (b)  $a_0 = 1 \text{ mm/s}^2$ , (c)  $a_0 = 1.7 \text{ mm/s}^2$ , (d)  $a_0 = 3 \text{ mm/s}^2$ , (e)  $a_0 = 6 \text{ mm/s}^2$ , displaced below Earth-Moon plane. The point A corresponds to the optimal displaced orbit.

In the rotating frame of reference, the condition for equilibrium solutions is obtained by setting  $\ddot{\mathbf{r}} = \dot{\mathbf{r}} = 0$  and we have the equality

$$\nabla \tilde{U}(\mathbf{r}) = \mathbf{a}, \quad (2)$$

where

$$\tilde{U}(\mathbf{r}) = - \left[ \frac{1}{2} |\boldsymbol{\omega}_* \times \mathbf{r}|^2 + \frac{GM}{r} \right],$$

where  $M$  is the mass of the Moon.

By making use of a set of cylindrical polar coordinates (see Figure 1 (a)), the two-body potential function  $\tilde{U}$  is given by

$$\tilde{U}(\rho, z; \omega_*) = - \left[ \frac{1}{2} (\omega_* \rho)^2 + \frac{GM}{r} \right]. \quad (3)$$

Then, the partial derivative of the potential  $\tilde{U}$  with respect to the position vector  $\mathbf{r} = (\rho, \phi, z)$  that will be needed for the stability analysis in the next section are given by

$$\frac{\partial \tilde{U}}{\partial \rho} = -\rho(\omega_{\star}^2 - \tilde{\omega}^2), \quad (4)$$

$$\frac{\partial \tilde{U}}{\partial \phi} = 0, \quad (5)$$

$$\frac{\partial \tilde{U}}{\partial z} = z\tilde{\omega}^2. \quad (6)$$

The equations of motion of the solar sail in component form may be written in cylindrical coordinates  $(\rho, z)$  as

$$\frac{GM}{r^2} \cos(\theta) = a_0 \cos^2(\gamma) \sin(\gamma), \quad (7)$$

$$\frac{GM}{r^2} \sin(\theta) - \omega_{\star}^2 \rho = a_0 \cos^3(\gamma), \quad (8)$$

with  $\cos(\theta) = \frac{z}{r}$ ,  $\sin(\theta) = \frac{\rho}{r}$ , where  $M$  is the mass of the Moon,  $G$  is the gravitational constant and the distance of the solar sail from the Moon is  $r = \sqrt{\rho^2 + z^2}$  so that

$$\frac{GMz}{r^3} = a_0 \cos^2(\gamma) \sin(\gamma), \quad (9)$$

$$\frac{GM\rho}{r^3} = a_0 \cos^3(\gamma) + \omega_{\star}^2 \rho. \quad (10)$$

Rearranging the equations (9) and (10), we obtain

$$\tan(\gamma) = \frac{z}{\rho} \left[ 1 - \left( \frac{\omega_{\star}}{\tilde{\omega}} \right)^2 \right]^{-1}, \quad (11)$$

for a given  $(\rho, z)$ , where

$$\tilde{\omega}^2 = \frac{GM}{r^3}. \quad (12)$$

Similarity from equations (9) and (10), the required radiation pressure acceleration for the two-body analysis may also be obtained as

$$a_0(\rho, z) = \cos^2(\gamma)^{-1} \left[ \left( (\tilde{\omega}^2 z)^2 + \left( \tilde{\omega}^2 \rho - \omega_{\star}^2 \rho \right)^2 \right)^{1/2} \right]. \quad (13)$$

With these conditions the spacecraft appears to execute a circular orbit displaced above or below the moon. Contours of required acceleration for a given  $(\rho, z)$  are shown in Figure 3 while the vector field describes the required sail orientation  $\mathbf{n}$ . The point marked A in Figure 3 represents the optimal displaced orbit (maximum displacement) for an acceleration  $a_0 = 1.7 \text{ mm/s}^2$ , equivalent to the orbit investigated by Ozimek et al.<sup>14</sup> Then, the linear stability properties of the families of orbits will now be investigated.

## ORBIT STABILITY

### Linearized system

The nonlinear equation of motion in the rotating of reference will now be linearised by adding a perturbation  $\sigma$  such that  $\mathbf{r} \rightarrow \bar{\mathbf{r}} + \sigma$ , where  $\bar{\mathbf{r}} = (\bar{\rho}, \bar{\phi}, \bar{z})$  corresponds to the nominal displaced non-Keplerian orbit solution. Then, the variational equation is obtained from the nonlinear equation of motion, Eq. (1) as

$$\ddot{\sigma} + 2\omega_* \times \dot{\sigma} + \Lambda\sigma = 0, \quad (14)$$

where

$$\Lambda = \left[ \frac{\partial \nabla \tilde{U}}{\partial \mathbf{r}} \right]_{\mathbf{r}=\bar{\mathbf{r}}}.$$

We define the perturbations in  $\bar{\mathbf{r}} = (\bar{\rho}, \bar{\phi}, \bar{z})$  as  $\sigma = (\xi, \psi, \eta)$ , so that Eq. (14) may be written as

$$\begin{bmatrix} \ddot{\xi} \\ \bar{\rho}\ddot{\psi} \\ \ddot{\eta} \end{bmatrix} + \begin{bmatrix} -2\omega_*\dot{\psi}\bar{\rho} \\ 2\omega_*\dot{\xi} \\ 0 \end{bmatrix} + \begin{bmatrix} \lambda_{11} & 0 & \lambda_{12} \\ 0 & 0 & 0 \\ \lambda_{21} & 0 & \lambda_{22} \end{bmatrix} \begin{bmatrix} \xi \\ \psi \\ \eta \end{bmatrix} = \begin{bmatrix} 0 \\ 0 \\ 0 \end{bmatrix}, \quad (15)$$

where  $\lambda_{11} = \tilde{U}_{\rho\rho}$ ,  $\lambda_{12} = \tilde{U}_{\rho z}$ ,  $\lambda_{21} = \tilde{U}_{z\rho}$  and  $\lambda_{22} = \tilde{U}_{zz}$ . By extracting the azimuthal terms from equation (15), it is found that

$$\bar{\rho}\ddot{\psi} + 2\omega_*\dot{\xi} = 0, \quad (16)$$

$$\ddot{\psi} + \frac{2\omega_*}{\bar{\rho}}\dot{\xi} = 0, \quad (17)$$

and Eq. (17) immediately integrates to

$$\dot{\psi} = -\frac{2\omega_*}{\bar{\rho}}\xi + C, \quad (18)$$

where  $C$  is a constant of integration.

By making use of Eq. (18), the first derivative terms from Eq. (15) will be removed to enable the variational equation to be written as

$$\begin{bmatrix} \ddot{\xi} \\ \ddot{\eta} \end{bmatrix} + \begin{bmatrix} \lambda_{11} & \lambda_{12} \\ \lambda_{21} & \lambda_{22} \end{bmatrix} \begin{bmatrix} \xi \\ \eta \end{bmatrix} = \begin{bmatrix} 2\omega_*C\bar{\rho} \\ 0 \end{bmatrix}. \quad (19)$$

In the following the bar notation is removed for clarity, so the matrix elements can be written as

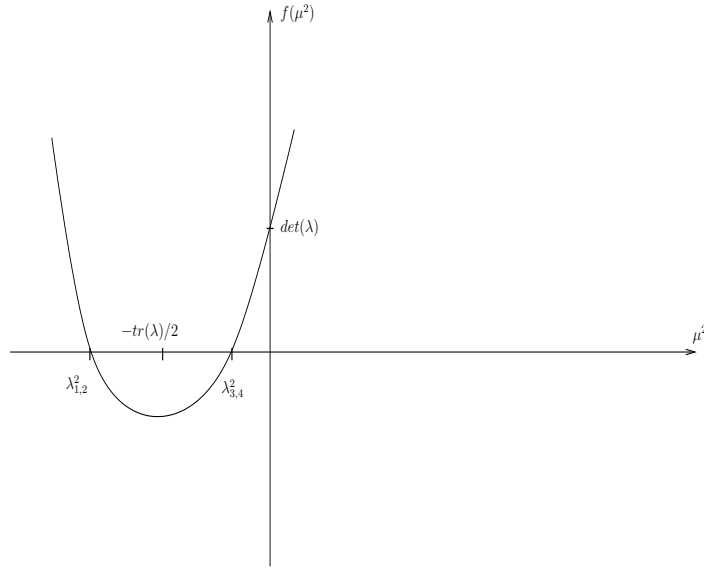


**Figure 4. Roots of the characteristic polynomial.**

$$\lambda_{11} = 3\omega_*^2 + \tilde{\omega}^2[1 - 3(\rho/r)^2], \quad (20)$$

$$\lambda_{12} = \lambda_{21} = -3\tilde{\omega}^2[\rho z/r^2], \quad (21)$$

$$\lambda_{22} = \tilde{\omega}^2[1 - 3(z/r)^2]. \quad (22)$$

Defining the transformation as

$$\xi = \xi' + \frac{2\omega_* C}{\lambda_{11}} \rho, \quad (23)$$

$$\eta = \eta', \quad (24)$$

a more familiar equation is then obtained if Eqs.(23) and (24) are substituted in the above expression (Eq. 19) to obtain

$$\begin{bmatrix} \ddot{\xi} \\ \ddot{\eta} \end{bmatrix} + \begin{bmatrix} \lambda_{11} & \lambda_{12} \\ \lambda_{12} & \lambda_{22} \end{bmatrix} \begin{bmatrix} \xi' \\ \eta' \end{bmatrix} = \begin{bmatrix} 0 \\ 0 \end{bmatrix}. \quad (25)$$

The stability characteristics of the approximate displaced two-body lunar orbits can be easily investigated by calculating the eigenvalues of the variational equation. Therefore, the eigenvalues may now be obtained by substituting an exponential solution of the form

$$\begin{bmatrix} \xi' \\ \eta' \end{bmatrix} = \begin{bmatrix} \xi_0 \\ \eta_0 \end{bmatrix} \exp(\mu t). \quad (26)$$

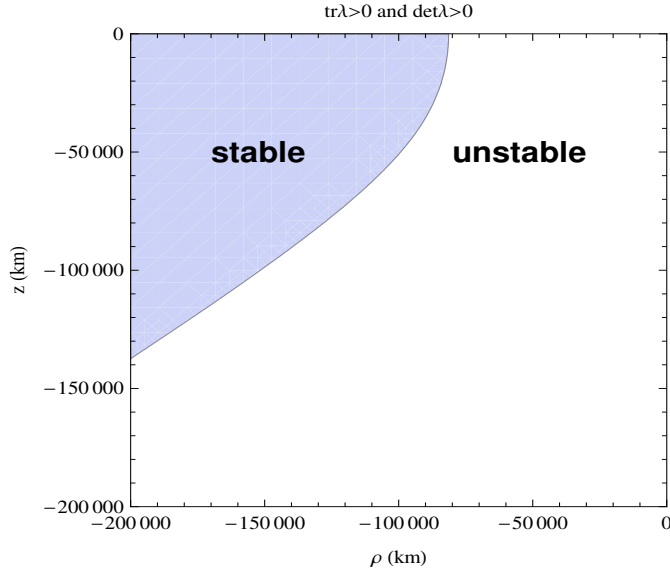


**Figure 5. Stable and unstable regions of the  $\rho$ - $z$  plane.**

Substituting this solution into Eq. (25) yields a matrix equation of the form

$$\begin{bmatrix} \mu^2 + \lambda_{11} & \lambda_{12} \\ \lambda_{12} & \mu^2 + \lambda_{22} \end{bmatrix} \begin{bmatrix} \xi_0 \\ \eta_0 \end{bmatrix} = \begin{bmatrix} 0 \\ 0 \end{bmatrix}. \quad (27)$$

The characteristic polynomial of the variational equation is then found to be

$$f(\mu^2) = \mu^4 + \mu^2(\lambda_{11} + \lambda_{22}) + (\lambda_{11}\lambda_{22} - \lambda_{12}^2), \quad (28)$$

and will be used to establish regions of linear stability and instability for approximate displaced two-body lunar orbits. The stability of the orbits depends on the properties of the characteristic equation given by Eq. (28). Thus, to guarantee nonpositive roots, and thus linear stability, it is required that the coefficients as well as the discriminant of the quadratic in  $\mu^2$  be positive. This can be shown to be true for displaced two-body lunar orbits in the case of the discriminant. By searching for regions with purely imaginary eigenvalues, we will determine the stability properties of displaced two-body lunar orbits. It is required that both  $\det(\lambda) = \lambda_{11}\lambda_{22} - \lambda_{12}^2 > 0$  and  $\text{tr}(\lambda) = \lambda_{11} + \lambda_{22} > 0$  for purely imaginary eigenvalues (see Figure 4). Then, it is found that

$$\lambda_{11} + \lambda_{12} = 3\omega_*^2 - \tilde{\omega}^2, \quad (29)$$

$$\lambda_{11}\lambda_{22} - \lambda_{12}^2 = \tilde{\omega}^2 \left[ 3\omega_*^2 \left( 1 - 3 \left( \frac{z}{r} \right)^2 \right) - 2\tilde{\omega}^2 \right]. \quad (30)$$

The first coefficient is strictly positive if

$$r > \sqrt[3]{\frac{GM}{3\omega_*^2}}. \quad (31)$$



In addition the second coefficient is strictly positive if

$$3\tilde{\omega}^2\omega_*^2\left(1 - 3\left(\frac{z}{r}\right)^2\right) - 2\tilde{\omega}^4 > 0. \quad (32)$$

For stable two-body approximation with  $z = 0$ , we have  $r > 81,360 \text{ km}$ , which lies well beyond the  $L_1$  point (see Figure (5)). It can be seen then that the family of approximate displaced two-body lunar orbits is partitioned into stable and unstable groups by the conditions  $\det(\lambda) > 0$  and  $\text{tr}(\lambda) > 0$  as shown in Figure (5).

We note now, due to the fact that the linearization is performed, the analysis of the stability provides only necessary conditions for stability and sufficient conditions for instability. In addition, we note that the model is an approximation to the full three-body problem.

## CONCLUSION

A previous study has shown the development of an asymptotic analysis for displaced lunar orbits. The displaced periodic orbits found approach the asymptotic solutions as the characteristic acceleration becomes large. In this paper, the problem concerning the linear stability for the Moon-Sail two-body approximation with constant radiation pressure has been investigated. A method was then developed to study the stability of the approximate displaced two-body lunar orbits. It was found that orbits with a large displacement are unstable.

## ACKNOWLEDGMENTS

This work was funded by the European Marie Curie Research Training Network, *AstroNet*, Contract Grant No. MRTN-CT-2006-035151 (J.S.) and European Research Council Grant 227571 VISIONSPACE (C.M.).

## REFERENCES

- [1] C. R. McInnes, *Solar sailing: technology, dynamics and mission applications*. London: Springer Praxis, 1999, pp. 11-29.
- [2] T. Waters and C. McInnes, "Periodic Orbits Above the Ecliptic in the Solar-Sail Restricted Three-Body Problem," *J. of Guidance, Control, and Dynamics*, Vol. 30, No. 3, 2007, pp. 687–693.
- [3] R. L. Forward, "Statite: A Spacecraft That Does Not Orbit," *Journal of Spacecraft and Rocket*, Vol. 28, No. 5, 1991, pp. 606–611.
- [4] V. Szebehely, *Theory of Orbits: the restricted problem of three bodies*. New York and London: Academic Press, 1967, pp. 497-525.
- [5] A. E. Roy, *Orbital Motion*. Bristol and Philadelphia: Institute of Physics Publishing, 2005, pp. 118-130.
- [6] F. Vonbun, "'A Humminbird for the  $L_2$  Lunar Libration Point'," *Nasa TN-D-4468*, April 1968.
- [7] G. Gómez, A. Jorba., J.Masdemont, and C. Simó, *Dynamics and Mission Design Near Libration Points*, Vol. IV. Singapore.New Jersey.London.Hong Kong: World Scientific Publishing Co.Pte.Ltd, 2001, Chap. 2.
- [8] R. Farquhar and A. Kamel, "Quasi-periodic orbits about the trans-lunar libration point," *Celestial Mechanics*, Vol. 7, 1973, pp. 458–473.
- [9] R. Farquhar, "The utilization of Halo orbits in advanced lunar operations," *Nasa technical report*, 1971.
- [10] J. Breakwell and J. Brown, "The 'halo' family of 3-dimensional periodic orbits in the Earth-Moon restricted 3-body problem," *Celestial Mechanics*, Vol. 20, 1979, pp. 389–404.
- [11] D. L. Richardson, "Halo orbit formulation for the ISEE-3 mission," *J. Guidance and Control*, Vol. 3, No. 6, 1980, pp. 543–548.
- [12] K. Howell, "Three-dimensional, periodic, 'halo' orbits," *Celestial Mechanics*, Vol. 32, 1984, pp. 53–71.

- [13] C. McInnes, "Solar sail Trajectories at the Lunar  $L_2$  Lagrange Point," *J. of Spacecraft and Rocket*, Vol. 30, No. 6, 1993, pp. 782–784.
- [14] M. Ozimek, D. Grebow, and K. Howell, "Solar Sails and Lunar South Pole Coverage," *In AIAA/AAS Astrodynamics Specialist Conference and Exhibit, AIAA Paper 2008-7080*, Honolulu, Hawaii, August 2008.
- [15] H. Baoyin and C. McInnes, "Solar sail orbits at artificial Sun-Earth Lagrange points," *Journal of Guidance, Control and Dynamics*, Vol. 28, No. 6, 2005, pp. 1328–1331.
- [16] C. R. McInnes, "Artificial Lagrange points for a non-perfect solar sail," *Journal of Guidance, Control and Dynamics*, Vol. 22, No. 1, 1999, pp. 185–187.
- [17] D. J. Scheeres, "Close Proximity Operations for Implementing Mitigation Strategies," *Planetary Defense Conference*, Orange County, California, 23<sup>rd</sup> Feb. 2004. AIAA 2004-1445.
- [18] C. McInnes, A. McDonald, J. Simmons, and E. McDonald, "Solar sail parking in restricted three-body systems," *Journal of Guidance, Control and Dynamics*, Vol. 17, No. 2, 1994, pp. 399–406.
- [19] J. Simo and C. R. McInnes, "Solar sail trajectories at the Earth-Moon Lagrange points," *In 59th International Astronautical Congress, IAC Paper 08.C1.3.13*, Glasgow, Scotland, 29 September - 03 October 2008.
- [20] J. Simo and C. R. McInnes, "Asymptotic Analysis of Displaced Lunar Orbits," *Journal of Guidance, Control and Dynamics*, Vol. 32, No. 5, September-October 2009, pp. 1666–1671.
- [21] C. McInnes, "The Existence and Stability of Families of Displaced Two-Body Orbits," *Celestial Mechanics and Dynamical Astronomy*, Vol. 67, No. 2, 1997, pp. 167–180.